Precise Indoor Positioning System for Mobile Robots via Smoothed UWB/IMU Sensor Fusion

Author(s): Elsanhoury, Mahmoud; Nieminen, Jyri; Välisuo, Petri; Siemuri, Akpojoto; Koljonen, Janne; Elmusrati, Mohammed; Kuusniemi, Heidi

Title: Precise Indoor Positioning System for Mobile Robots via Smoothed UWB/IMU Sensor Fusion

Year: 2023

Version: Acccepted manuscript

Please cite the original version:

Elsanhoury, M., Nieminen, J., Välisuo, P., Siemuri, A., Koljonen, J., Elmusrati, M. & Kuusniemi, H. (2023). Precise Indoor Positioning System for Mobile Robots via Smoothed UWB/IMU Sensor Fusion. In *2023 13th International Conference on Indoor Positioning and Indoor Navigation (IPIN)*. IEEE. https://doi.org/10.1109/IPIN57070.2023.10332542

Precise Indoor Positioning System for Mobile Robots via Smoothed UWB/IMU Sensor Fusion

Mahmoud Elsanhoury
Digital Economy Platform
University of Vaasa
Vaasa, Finland
0000-0002-9195-4613
first.lastname@uwasa.fi

Jyri Nieminen
VEBIC Platform
Digital Economy Platform
University of Vaasa
Vaasa, Finland
0009-0001-5477-3792
first.lastname@uwasa.fi

Petri Välisuo
School of Technology and Innovations
Digital Economy Platform
University of Vaasa
Vaasa, Finland
0000-0002-9566-6408
first.lastname@uwasa.fi

Akpojoto Siemuri
Digital Economy Platform
University of Vaasa
Vaasa, Finland
0000-0002-2644-1985
first.lastname@uwasa.fi

Janne Koljonen
School of Technology and Innovations
University of Vaasa
Vaasa, Finland
0000-0001-5834-4437
first.lastname@uwasa.fi

Mohammed Elmusrati
School of Technology and Innovations
University of Vaasa
Vaasa, Finland
0000-0001-9304-6590
first.lastname@uwasa.fi

Heidi Kuusniemi
Digital Economy Platform
School of Technology and Innovations
University of Vaasa
Vaasa, Finland
0000-0002-7551-9531
first.lastname@uwasa.fi

***Abstract*—Indoor positioning systems (IPSs) are the foundations for all indoor location-based services and applications. In this article, we present a precise and robust IPS using ultra wide-band (UWB) technology fused with an inertial measurement unit (IMU). Both technologies are integrated to account for the non line of sight (NLOS) problems arising in a dense challenging environment found within an industrial laboratory in Finland. Besides the conventional estimation techniques e.g. extended Kalman filter (EKF), we employ the Rauch-Tung-Striebel (RTS) smoothing algorithm in addition to a multivariate regression-based offset compensation method to improve the overall positioning accuracy of the system. The recommended number of distributed UWB anchors versus the coverage area is also discussed and tested in this article. The experiments were held by a patrolling mobile robot with millimeter accuracy, which acted as a ground truth reference to all used algorithms. The positioning estimation results showed a superior performance by the proposed method (UWB/IMU EKF-RTS-LR) with mean accuracy of 4.7 cm, and 9.6 cm for more than 95% of the time.**

***Index Terms*—indoor positioning system (IPS), mobile robots, ultra-wideband (UWB), sensor fusion, inertial motion unit (IMU)**

I. Introduction

Indoor positioning systems (IPSs) play an important role in Industry 4.0 and Internet of Things (IoT) applications. They are the backbone of all indoor navigational and location-based applications found in e.g. smart logistics, asset tracking, smart manufacturing, healthcare applications, smart delivery, etc [1], [2]. However, IPSs face many challenges from various aspects. Primarily, a reliable IPS should achieve an acceptable level in performance metrics such as accuracy, availability, continuity, and integrity [3]. That is why, a reliable IPS usually imposes heavy costs for meeting all metrics to sufficient degrees, especially for certain sensitive applications such as smart manufacturing (e.g. forgery and 3D printing), and healthcare location-based equipment. Moreover, IPSs suffer from discontinuities especially the wireless-based technologies that are highly affected by the impairments of the propagation channel in addition to the blockage and signal denial in some environments, a problem that is very common in the IPS domain.

Fortunately, recent researches affirm that low-cost reliable positioning is feasible by employing one or more assisting resources to aid the primary IPS technology [4]. Thus, a reliable IPS is not necessarily dependent on a single technology, rather, multiple technologies could be fused together to complement the desired performance metrics and achieve reliable positioning estimations.

Sensor fusion is an integration of two or more technologies via computational methodologies that are bound by fusion algorithms such that the output information is maximized [5]. By nature, sensors are prone to systematic errors, biases, and drifts, consequently, sensor fusion methods help in the mitigation of errors as much as possible.

Within the campus of our research institute, the University of Vaasa, lies the reputable industrial venue of Technobothnia, a modern laboratory that serves a minimum of five universities in addition to numerous corporations in the region. This industrial venue consists of several laboratories for all kinds of technical sciences e.g. industrial robotics, smart operations, mobile robots, chemistry labs, heavy-duty 3D printing machines, telecommunications equipment, etc. The visiting traffic is high, hence, an indoor positioning system will be very beneficial to both human operators and robot assets inside the lab. However, the allocated resources are limited to low-cost IPS systems that are based on wireless technologies e.g. ultra wide-band (UWB), Wi-Fi, Bluetooth low energy (BLE). An UWB system and an inertial measurement unit (IMU) are selected as the elements of the precise IPS in Technobothnia, with UWB as the primary technology, and IMU as the assisting sensor fusion unit. For later use, Wi-Fi and BLE were considered for future imprecise IPSs that shall track assets within 2-3 meters of accuracy.

The fusion of UWB/IMU is abundant in recent IPS literature. Ali *et.al.* showed that the UWB-IMU combination with adaptive Kalman Filter can be used for precision pedestrian positioning even in occasional non line of sight (NLOS) situations [6]. Additional smoothing methods have been shown to improve the precision of the UWB/IMU fusion based positioning in some cases [7]. UWB/IMU positioning can be also fused with many other sensors, such as cellular phone signals, to increase the positioning accuracy and robustness [8]. With fault-tolerant additions, the UWB/IMU combination can be used in demanding mission-critical environments such as coal mines [9], [10]. A more detailed literature review about fusion-based positioning (focusing on UWB/IMU integration) is presented in [2].

The rest of article is organized as follows: Section II describes the main objectives of this research, and the essential embedded elements (software and hardware) to build the IPS system. Section III explains more aspects about the methodology, devices configurations, and the overall setup of the environment. Section IV discusses the output results and provides technical interpretations, evaluations, and commentaries on the applied performance metrics. Followed by a "Conclusion" section to highlight the achievements and potential future work.

II. Fusion Technique

The main objective in this study, is to achieve a reliable IPS with the most possible degree of precision positioning for mobile robots inside the industrial laboratory of Technobothnia, situated in Vaasa - Finland. Since the environment is dense and challenging, the solution had to be through the multisensor fusion technique to keep the overall cost under the budget limits allocated for the IPS. As described in [2], a low-cost system can be built from a single precise wireless technology such as UWB then fused with an assisting technology, that is, IMU to correct the biased, missing, and null values caused by NLOS conditions especially in dense environments. Thus, a loosely-coupled UWB/IMU integrated scheme was implemented as a precise IPS for mobile robots in the selected venue. A floor plan of the experiment area at Technobothnia laboratory is illustrated in Figure 1.

A. Positioning sensors

A Decawave laboratory kit MDEK1001 [11] was utilized to build the UWB positioning system inside our industrial laboratory environment, Technobothnia. Our setup for the MDEK1001 system consisted of one movable tag, and 6 evenly distributed anchors to cover the experimental area of 28x15 squared meters evenly, an additional seventh anchor

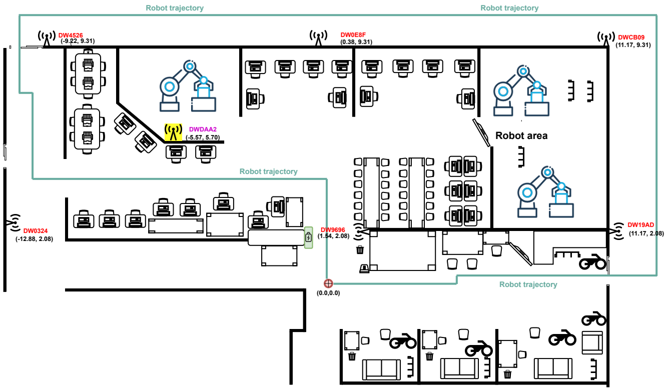

Fig. 1. Floor plan of Technobothnia laboratory with the planned robot trajectory. The highlighted location (yellow) is reserved for the tentative seventh UWB anchor. Battery-like block refers to the robot's docking station.

(DAA2) was inserted at some point to investigate the performance of 6 Vs 7 anchors and the effect of adding more anchors to the setup, which will be discussed in the results sections. The default settings of the Decawave kit are programmed to provide raw distance measurements between the moving tag and a maximum of four anchors (constrains from Decawave) based on the time of arrival (ToA) two-way ranging (TWR) technique, in addition to providing the final EKF estimates of the tag position [11].

Besides, an inertial measurement unit (IMU) sensor Xsens MTi-630 was used to obtain the inertial data of the movable robot such as: orientation, rate of turn, acceleration, and magnetism. The IMU sensor provided another layer of information about the movement of the robot inside the dense environment, thus, accounting for the NLOS situations and helping in inferring the missing data to improve the output fusion-based positioning estimations.

Both UWB and IMU sensors were placed onboard an autonomous mobile robot developed by OMRON (as shown in Figure 2), which possesses numerous positioning sensors such as: LASERs, ultrasound, RADARs, IMU, and LiDARs. The positioning data obtained from the OMRON robot had a millimeter accuracy with a confidence score of more than 90% most of the time (as stated by the built-in robot controller system), hence, it acted as the reference ground truth to our UWB/IMU fusion system.

As shown in Figure 1, a dense industrial environment comprising robots, metallic structures, and concrete materials was selected to test our hypothetical approach for precise indoor fusion-based positioning. The co-ordinal locations of the six UWB anchors are evenly distributed around the venue (area: 28x15 square meters), the seventh UWB anchor highlighted in yellow, was inserted to check the sufficiency of using 6 Vs 7 anchors. The planned robot trajectory was selected to be a multi-modal route i.e. mixed paths of clear and obscured lines of sight (LOS) between the user tag and the fixed anchors, to test the reliability of the system in complex conditions.

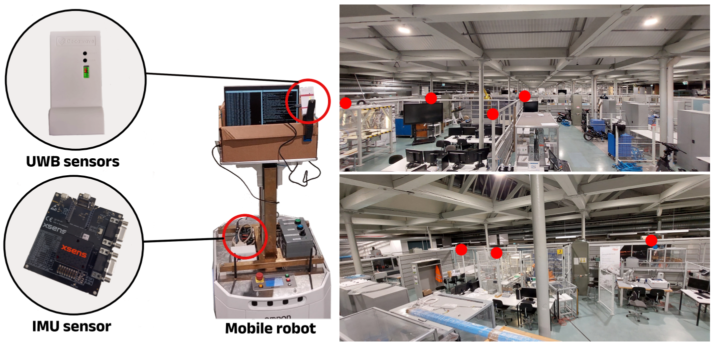

Fig. 2. Embedded elements of the designed IPS showing UWB anchors and tag (Decawave), IMU sensor (XSENS), the fusion software (laptop), and the mobile robot (OMRON). The red dots refer to the locations of fixed UWB anchors, including an additional spot for the tentative seventh anchor.

B. Algorithms

A set of algorithms was selected and applied to sensor readings locally (per sensor) and globally (fusion) in order to achieve more accurate positioning estimations.

1) Dead Reckoning (DR): is widely used in positioning and navigation applications even before the invention of modern localization systems, nowadays the most well-known implementation of DR is the pedestrian dead reckoning (PDR) algorithm which is employed in numerous location-based applications. In this method, we utilized the DR algorithm to fix the blank and null values arriving from UWB sensor readings by incorporating the previous non-null values and the heading angle into the DR estimation of the current missing epoch, as illustrated in Equations (1).

$$
\begin{aligned}
D_k &= \sqrt{(p^x_{k-2} - p^x_{k-1})^2 + (p^y_{k-2} - p^y_{k-1})^2} \\
\phi_k &= \text{arctan2}\left(\frac{p^y_{k-2} - p^y_{k-1}}{p^x_{k-2} - p^x_{k-1}}\right) \\
p^x_k &= p^x_{k-1} + D_k \cos(\phi_k) \\
p^y_k &= p^y_{k-1} + D_k \sin(\phi_k)
\end{aligned}
\tag{1}
$$

where p^x_k and p^y_k are the x-y positions at time instant k, D_k and ϕ_k are the calculated Euclidean distance and the heading angle from the previous two x-y positions, respectively.

2) Extended Kalman Filter (EKF): is a nonlinear state-space estimation algorithm that is typically used for 2-D and 3-D positioning estimations. In Decawave UWB devices, the system already contains a built-in EKF module that outputs the final filtered data after processing raw ToA measurements from anchors. However, UWB readings are fluctuating around a mean value, which requires further filtration. To this aim, the output positioning values from the Decawave system are fused with the data from the IMU sensor to mitigate the residuals via another layer of EKF Fusion algorithm that combines both information. EKF algorithm proceeds with two steps: the **prediction** step where the prior state mean and covariance are predicted before checking the measurements vector, and the **update** step in which the posterior state mean and covariance are updated after checking the measurements vector. The complete set of formulas employed for the fusion is shown in Equations (2) [12].

$$
\begin{aligned}
m_k^- &= f(m_{k-1}, k-1) \\
P_k^- &= F_x\, P_{k-1} {F_x}^T + Q_{k-1} \\
V_k &= y_k - h(m_k^-, k) \\
S_k &= H_x\ P_k^-\ {H_x}^T + R_k \\
K_k &= P_k^-\ {H_x}^T\ S_k^{-1} \\
m_k &= m_k^- + K_k V_k \\
P_k &= P_k^- - K_k S_k K_k^T
\end{aligned}
\tag{2}
$$

where $m_{\bar{k}}$ and $P_{\bar{k}}$ are the prior state predicted mean and covariance at time instant k, respectively, m_k and P_k are the posterior state estimated mean and covariance. y_k is the measurements vector at time instant k, and S_k is the measurement prediction covariance. K_k is the filter gain, $f(.)$ and $h(.)$ are the dynamic nonlinear functions of the state-space model and the measurements model, respectively.

For the EKF fusion filter, the state-space vector $\mathbf{x_k}$ comprises the x-y positions, velocities, and accelerations (i.e. 2-D Wiener dynamic model). While, the measurements vector $\mathbf{y_k}$ includes the x-y positions inbound from Decawave devices, the x-y accelerations and the heading angles inbound from the IMU sensor.

3) Rauch-Tung-Striebel (RTS) Smoother: is a Bayesian recursive filter that smoothens the linearized state-space estimates by considering the maximum likelihood of the probability density function (mean and covariance), which are smoothed retroactively [12], [13].

The prior and posterior states estimates $\hat{X}_k|k-1, \hat{X}_k|k$ and their covariances $\hat{P}_k|k-1, \hat{P}_k|k$ which were obtained from the EKF fusion filter are fed to the RTS smoother to calculate the smoothed state estimates $\hat{X}_k|n$, and covariance $\hat{P}_k|n$. The RTS smoother formulas are described in Equations (3) [12], [13].

$$
\begin{aligned}
\hat{X}_k|_n &= \hat{X}_k|_k + C_k(\hat{X}_{k+1}|_n - \hat{X}_{k+1}|_k) \\
P_k|_n &= P_k|_k + C_k(\hat{X}_{k+1}|_n - \hat{X}_{k+1}|_k) \times C_k^T
\end{aligned}
\tag{3}
$$

where $C_k = P_k|_k F^T_{k+1} P^{-1}_{k+1}|_k$, and $X_k|_k$ is the a-posterior state estimate of time instant k and $X_{k+1}|_k$ is the a-prior state estimate of time instant $k+1$ which also applies to the covariance.

4) Linear Regression (LR) Model: is a statistical method that is used for predictive analysis. It is one of the most common types of supervised machine learning algorithms used to compute the linear relationship between the dependent variable(s) and one or more independent features [14]. Generally, the linear regression function is represented as seen in Equation (4).

$$Y = m + X \times b \tag{4}$$

In the hypothesis function for multivariate linear regression, we assumed that the independent features are the Cartesian [x, y] values of the OMRON robot and UWB respectively, which are represented by X in Equation (4). And, the respective offsets between the OMRON robot (which provides the ground truth data) and UWB represented by Y in Equation (4), is the dependent variable. Assuming there is a linear relationship between X and Y then the offsets can be predicted using Equation (5):

$$y_i = m + \sum_{j=1}^{n} x_{i,j}\beta_j + \epsilon \tag{5}$$

where $i = 1, 2 \dots n$, and $y_i \in Y$ is the dependent variable, $x_{i,j} \in X$ are the independent variables (multiple inputs, $j = 1, 2 \dots m$), and ϵ is the prediction error.

The model gets the best regression fit by finding the best m and β_j values where m is the intercept and β_j is the coefficient of $x_{i,j}$. The mean squared error (MSE) is used as the cost (loss) function L, in order to compute the error, which is the difference between the predicted value $\hat{y}$ and the true value y. The loss function $L(\Theta)$ can be written as in Equation (6):

$$L(\Theta) = \frac{1}{n}\sum_{i=1}^{n}(\hat{y}_i - y_i)^2 \tag{6}$$

A flowchart describing the sequence of utilizing all the above-mentioned algorithms is shown in Figure 3.

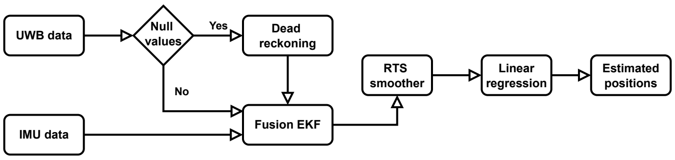

Fig. 3. Sequence of utilized algorithms.

III. Experimental setup

To set the scene for testing our hypothetical UWB/IMU fusion positioning system in the selected venue, a complete customized embedded system was built that comprises the essential software and hardware peripherals. Then, the devices and the targeted environment were setup for experimentation.

A. Hardware and software

The hardware part consists of a distributed set of six UWB anchors (Decawave) with fixed positions around the coverage area, the IMU sensor (XSENS) mounted on the mobile robot, and the robot itself (OMRON), as shown in Figure 2.

The software part comprises numerous code files that record and communicate real-time data to a storage server. Every sensor point (UWB, IMU, and robot) has a dedicated software scanner that collects the desired tensors of data with the appropriate settings for their units. Afterward, the scanner passes them over to the NodeRed server via web sockets, eventually, they are stored in a local web server which is managed by our institute (i.e. the user), as illustrated in Figure 4.

The Wi-Fi and BLE scanners are already developed but reserved for future use, the focus of this article is centered around UWB/IMU fusion.

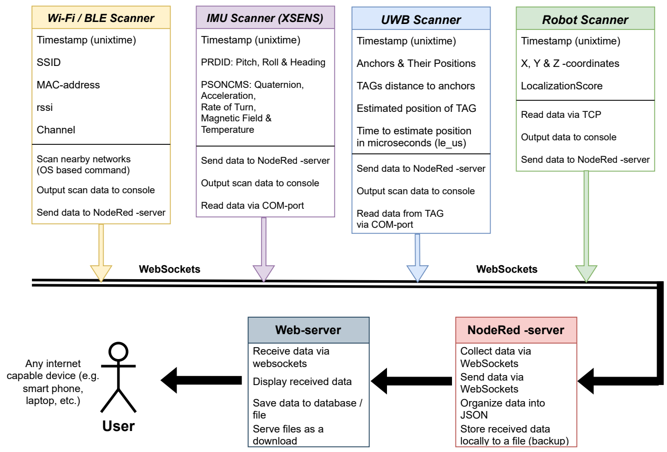

Fig. 4. Block diagram showing the scheme of sensors data collection.

B. Calibration and configuration

All sides of the coverage area including the locations of the fixed UWB anchors were laser-metered using a highly accurate LASER ranger, the measurements were repeated several times till they were sufficiently verified (i.e. standard deviation was $\leq$ 0.01 m). The sensors of the robot were calibrated with localization accuracy exceeding 90% score (as stated by the built-in robot positioning system called "Mobile Runner"), in addition to surveying a new high-detail map of the surrounding environment with updated furniture positions. UWB and IMU sensors were calibrated and configured to produce the appropriate units and positioning output, furthermore, the origin points of all sensors were aligned into a single origin point explicitly marked on the laboratory floor and programmed into sensor configurations. All sensors (UWB, IMU, and robot) were configured to a sample rate of 10 Hz (Ts = 0.1 second).

C. Route design

On the robot's software controller (Mobile Runner), specific routes were designed to allow the robot to patrol the coverage area in various situations: 1) clear LOS with the robot, 2) poor LOS, 3) visibility through concrete and metal structures, and 4) with the fewest number of anchors (three) visible to the robot. Consequently, six UWB anchor locations were selected to provide evenly distributed coverage to the robot, a seventh location was reserved for a feasibility test.

With all concerns addressed and systems configured, the environment became ready for testing.

IV. Results and discussion

As shown in Figure 5, a dedicated graph for every step (i.e. raw UWB measurements, EKF fusion, RTS smoothing, and LR filtration) is rendered to analyze and assess the proposed method for both configurations scenarios (6 Vs 7 anchors). In addition, a cumulative distribution function (CDF) curve per algorithm is sketched to investigate the performance of the system for longer periods. Moreover, Tables I and II show the mean absolute error (MAE), root mean square error (RMSE), and the 95% percentile values for all algorithms in both scenarios.

TABLE I
Positioning errors [meters] when 6 UWB anchors are used

	UWB	+Fusion	+RTS	+LR
MAE	0.240	0.259	0.232	0.078
RMSE	0.417	0.445	0.389	0.088
p95%	0.278	0.243	0.267	0.141

TABLE II
Positioning errors [meters] when 7 UWB anchors are used

	UWB	+Fusion	+RTS	+LR
MAE	0.221	0.235	0.218	0.047
RMSE	0.323	0.344	0.319	0.055
p95%	0.413	0.340	0.386	0.096

From Figure 5, it is noticeable that the unprocessed UWB measurements are having moderate accuracy with noticeable errors around the start and the stop positions which both have maximum fluctuations in the data, especially from the 6-anchors configuration. Meanwhile, the EKF fusion-based positioning algorithm is performing slightly poorer than the raw UWB data, this remark is also fortified by checking the CDF in the below subplot where the EKF fusion algorithm is found to be the least accurate on the long term without receiving assistance from the RTS smoother algorithm. Consequently, higher accuracy is achieved by backing the EKF fusion algorithm with RTS smoother algorithm, which yielded significantly higher accuracy than the performance of the EKF fusion algorithm, while having slightly higher accuracy than the raw UWB measurements, as also asserted by the numerical values of MAE, RMSE, and p95% in Table I.

The model of LR algorithm was previously trained using positioning data recorded by the OMRON robot from the same environment (but different dataset values), and been used as a training data for the algorithm to both scenarios. Hence, the best positioning accuracy for the 6-anchor configuration is achieved by smoothing the output of the EKF-RTS algorithm with LR algorithm, the procedure that not only helped in improving the performance of the IPS but also achieved significantly precise positioning results as seen from both Figure 5 and Table I. LR filtration step yielded the best positioning accuracy in the 6-anchor configuration data with MAE = 7.8 cm, and RMSE = 8.8 cm compared to the second best records of 23.2 cm (RTS MAE), and 38.9 cm (RTS RMSE), respectively. Furthermore, the long term performance of the UWB/IMU EKF-RTS-LR algorithm is the highest ever in the 6-anchors configuration, by achieving 95% percentile value of 14.1 cm (could have been better if the stationary fluctuations were mitigated) and the most steep curve in the CDF plot, meaning that the LR smoothed solution is the best candidate for continuous accurate navigation services with relatively high standards for an IPS in this dense environment.

On the other hand, the positioning results from the 7-anchor configuration are found to be more promising in most performance metrics as the positioning errors from all methods are more improved than the 6-anchor configuration. Firstly, the EKF fusion continue to perform slightly poorer than the raw UWB measurements and all other algorithms, as seen from the 2nd and 4th subplots of Figure 5, and the values from Table II. Similar to the 6-anchor configuration, the RTS smoothed EKF fusion results are coping with the raw UWB measurements most of the time, but outperform them in few occasions, that is why the CDF curve, MAE, RMSE, and p95% values of both algorithms are nearly identical.

Finally, the ultimate method that comprises UWB/IMU EKF-RTS-LR possesses the best performance metrics in the 7-anchor configuration too, which was an expected behaviour from the algorithm. The LR filtration step had leveraged the overall methodology to achieve MAE = 4.7 cm, and RMSE = 5.5 cm only, which is -by far- the most precise positioning accuracy ever achieved in the Technobothnia lab environment. The second most precise results were -again- from the RTS smoother of MAE = 21.8 cm, and RMSE = 31.9 cm. In addition, the long term performance of the UWB/IMU EKF-RTS-LR algorithm in the 7-anchors configuration is found to be also the highest with p95% = 9.6 cm and the steepest CDF plot among all other algorithms.

In summary, the LR smoothed EKF-RTS fusion algorithm can help to achieve the most precise positioning estimations inside Technobothnia laboratory, since it has demonstrated significantly better MAE, RMSE, and p95% values than all other algorithms, meaning that it does not only have the capability to achieve the most accurate positioning but will also score acceptable levels of continuity, availability and integrity. Thus, the recommended configuration is to cover the given region with 7 UWB anchors aided by the UWB/IMU EKF-RTS-LR algorithm to achieve precise positioning estimations for a mobile robot activity in dense industrial environments as Technobothnia lab, Finland.

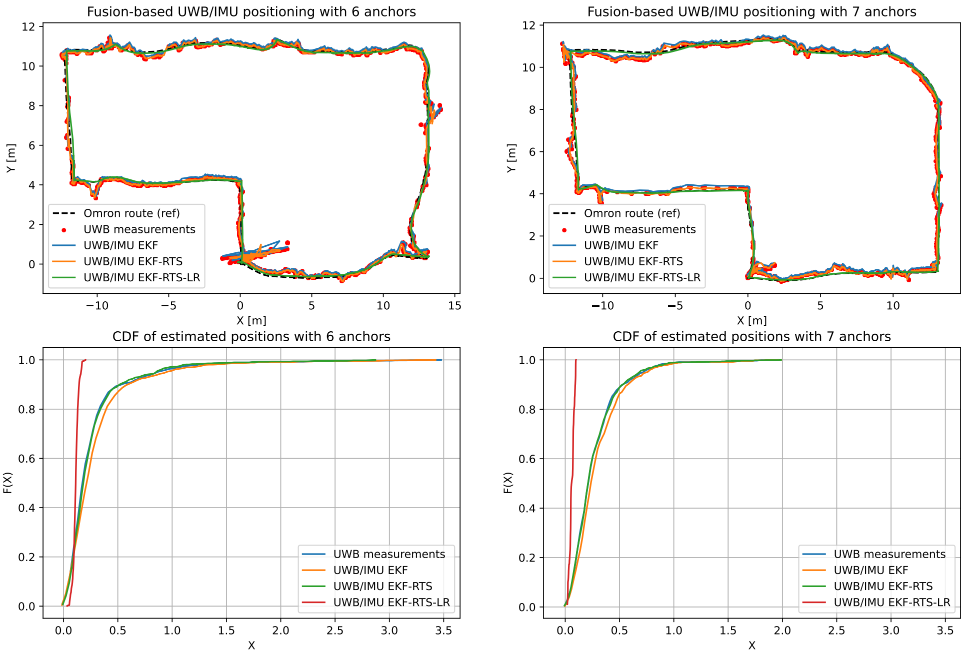

Fig. 5. Plots showing the final positioning results from all utilized algorithms in both configuration scenarios (6 Vs 7 anchors). The lower subplots show the corresponding CDF curves for all algorithms in every scenario.

V. Conclusions

Precise indoor positioning systems are crucial for indoor mobile robot operations especially in dense industrial environments. In this article, we demonstrated our realization of the proposed IPS to provide precise positioning estimations for indoor activities. Through the loosely-coupled multisensor fusion scheme of UWB/IMU technologies and the use of EKF/RTS/LR smoothing algorithms, our method has achieved a positioning accuracy of 9.6 cm across 95% of the time, that is a mean absolute error of 4.7 cm (RMSE = 5.5 cm), using seven UWB anchors to cover a robot operation area of 28x15 square meters in a dense challenging environment. For future work, we aim at investigating more aspects to improve the IPS performance in addition to test RSS-based positioning systems (Wi-Fi and BLE) in the same environment.

Acknowledgment

This work is supported by TULEVA and TosiPaikka projects funds. The corresponding author would like to thank Mrs. Mai Moustafa (Architectural engineer – City of Vaasa) for refurbishing some of the illustrative figures within this article.

References

[1] A. Alarifi, A. Al-Salman, M. Alsaleh, A. Alnafessah, S. Al-Hadhrami, M. Al-Ammar, and H. Al-Khalifa, "Ultra Wideband Indoor Positioning Technologies: Analysis and Recent Advances," *Sensors*, vol. 16, p. 707, may 2016.

[2] M. Elsanhoury, P. Mäkelä, J. Koljonen, P. Välisuo, A. Shamsuzzoha, T. Mantere, M. Elmusrati, and H. Kuusniemi, "Precision positioning for smart logistics using ultra-wideband technology-based indoor navigation: A review," *IEEE Access*, vol. 10, pp. 44413–44445, 2022.

[3] N. Zhu, J. Marais, D. Bétaille, and M. Berbineau, "Gnss position integrity in urban environments: A review of literature," *IEEE Transactions on Intelligent Transportation Systems*, vol. 19, no. 9, pp. 2762–2778, 2018.

[4] X. Guo, N. Ansari, F. Hu, Y. Shao, N. R. Elikplim, and L. Li, "A Survey on Fusion-Based Indoor Positioning," *IEEE Communications Surveys & Tutorials*, vol. 22, no. 1, pp. 566–594, 2020.

[5] M. Elsanhoury, J. Koljonen, P. Välisuo, M. Elmusrati, and H. Kuusniemi, "Survey on recent advances in integrated GNSSs towards seamless navigation using multi-sensor fusion technology," in *Proceedings of the 34th International Technical Meeting of the Satellite Division of The Institute of Navigation (ION GNSS+ 2021)*, Institute of Navigation, Oct. 2021.

[6] R. Ali, R. Liu, A. Nayyar, B. Qureshi, and Z. Cao, "Tightly Coupling Fusion of UWB Ranging and IMU Pedestrian Dead Reckoning for Indoor Localization," *IEEE Access*, vol. 9, pp. 164206–164222, 2021.

[7] D. Feng, C. Wang, C. He, Y. Zhuang, and X.-G. Xia, "Kalman-Filter-Based Integration of IMU and UWB for High-Accuracy Indoor Positioning and Navigation," *IEEE Internet of Things Journal*, vol. 7, pp. 3133–3146, Apr. 2020.

[8] C.-S. Jao, A. A. Abdallah, C. Chen, M.-W. Seo, S. S. Kia, Z. M. Kassas, and A. M. Shkel, "PINDOC: Pedestrian Indoor Navigation System Integrating Deterministic, Opportunistic, and Cooperative Functionalities," *IEEE Sensors Journal*, vol. 22, pp. 14424–14435, July 2022.

[9] H. Yang, T. Luo, W. Li, L. Li, Y. Rao, and C. Luo, "A Stable SINS/UWB Integrated Positioning Method of Shearer Based on the Multi-Model Intelligent Switching Algorithm," *IEEE Access*, vol. 7, pp. 29128–29138, 2019.

[10] M.-G. Li, H. Zhu, S.-Z. You, and C.-Q. Tang, "UWB-Based Localization System Aided With Inertial Sensor for Underground Coal Mine Applications," *IEEE Sensors Journal*, vol. 20, pp. 6652–6669, jun 2020.

[11] Decawave, "Mdek1001 kit user manual module development & evaluation kit for the dwm1001," 2017.

[12] J. Hartikainen, A. Solin, and S. Särkkä, *Optimal filtering with Kalman filters and smoothers - a Manual for Matlab toolbox EKF/UKF*. Aalto University, 2011.

[13] H. E. Rauch, F. Tung, and C. T. Striebel, "Maximum likelihood estimates of linear dynamic systems," *AIAA Journal*, vol. 3, no. 8, pp. 1445–1450, 1965.

[14] K. Kumari and S. Yadav, "Linear regression analysis study," *Journal of the Practice of Cardiovascular Sciences*, vol. 4, p. 33, 01 2018.